Foundation are gratefully acknowledged for financial support.

Registry No. 1, 35344-11-7; 2, 89875-17-2; 4, 100197-93-1; 5, 79001-07-3; 6, 125475-95-8; 7, 125475-96-9; 8, 125475-97-0; 9, 86744-25-4; 10, 125475-98-1; 12, 99324-46-6; 13a, 125476-00-8; 13b, 125475-99-2; $ClCH_2OCH_3$, 107-30-2; $Me_3SiOSO_2CF_3$, 27607-77-8.

Supplementary Material Available: Tables of positional parameters and their estimated standard deviations, complete listings of bond distances and angles, refined displacement parameter expressions, and root-mean-square amplitudes of thermal vibration for 4 (9 pages); a listing of observed and calculated structure factors for 4 (11 pages). Ordering information is given on any current masthead page.

Reaction of CH_2O with $[Co(PMe_3)_4]X$ (X = PF_6 and BPh_4). Structural Characterization of $[Co(CO)(PMe_3)_4]PF_6$ and the Nonstoichiometric Complex $[CoH_{2-2x}(CO)_x(PMe_3)_4]BPh_4$

Yolande Pérès, Michèle Dartiguenave,* and Yves Dartiguenave

Laboratoire de Chimie de Coordination, 205 route de Narbonne, 31077 Toulouse Cedex, France

James F. Britten and André L. Beauchamp*

Département de Chimie, Université de Montréal, C.P. 6128, Succ. A, Montréal, Québec, Canada H3C 3J7

Received August 2, 1989

$[Co(PMe_3)_4]PF_6$ reacts with formaldehyde to form $[Co(CO)(PMe_3)_4]PF_6$, which is shown by X-ray diffraction ($P2_1/n$, a = 11.280, b 14.948, c = 14.088 Å, β = 90.69°, Z = 4, R = 0.029) to contain trigonal-bipyramidal cations with CO in the *equatorial* position. From $[Co(PMe_3)_4]BPh_4$, $[Co(CO)(PMe_3)_4]BPh_4$ is formed in low yield. The major product is crystallographically characterized ($P2_1$, a = 15.985, b = 12.512, c = 20.410 Å, β = 111.76 (3)°, Z = 4, R = 0.048) and found to contain the cis-octahedral Co(III) dihydrido species $[CoH_2(PMe_3)_4]^+$ and the Co(I) cation $[Co(CO)(PMe_3)_4]^+$ with CO in the *axial* position. These two ions are disordered over the cationic sites in the crystal. The presence of these species in the nonstoichiometric material is also indicated by infrared and NMR data on the compound and its ^2H- and ^{13}C-labeled derivatives.

Introduction

The synthesis and decomposition mechanisms of d^8 metal complexes containing formyl groups, hydroxymethyl groups, carbon monoxide, or formyl-derived methyl groups still attract considerable attention in connection with the role of such species as intermediates in carbon monoxide hydrogenation promoted by homogeneous or heterogeneous catalysts.[1-3] Studies conducted by Thorn et al. on the reaction of CH_2O with cationic $[M(PMe_3)_4]X$ compounds have led to the preparation of the first cationic formyl compound $[MH(CHO)(PMe_3)_4]X$ with M = Ir, but only the carbonyl species has been obtained for M = Rh.[2] With ruthenium and osmium, Roper et al. have isolated molecular formaldehyde and formyl complexes.[4,5] Nickel(0)–phosphine $Ni(PR_3)_4$ complexes have been found to promote the decomposition of formaldehyde into CO and H_2 with formation of $Ni(CO)(PR_3)_3$.[6] No reactions have been performed so far on the cobalt analogues, but for hydroformylation, modifying the $Co_2(CO)_8$ catalyst by addition of phosphines of small cone angle increased the proportion of formate obtained.[7] We felt that the basic coordination chemistry of the cobalt system toward CH_2O had to be examined in greater detail. We wish to report our results on the reaction of CH_2O with $[Co(PMe_3)_4]X$ for X = PF_6 and BPh_4. Interestingly, the chemistry of this system was found to be dependent on the counterion used, and it allowed us to observe both the axial-CO and equatorial-CO forms of the trigonal-bipyramidal $[Co(CO)(PMe_3)_4]^+$ ion.

Experimental Section

Materials and Methods. Solvent distillation and all other operations were carried out under argon by using standard Schlenk techniques. Tetrahydrofuran was distilled over Na/benzophenone just before use. Methanol and acetonitrile were distilled over molecular sieves. All solvents were degassed by three freeze–thaw cycles. Trimethylphosphine[8] and $CoBr(PMe_3)_3$[9] were prepared by literature methods. Paraformaldehyde and aqueous formaldehyde (stabilized with 10% methanol) were used without further purification. [^2H]- and [^{13}C]paraformaldehyde (CEA) were used as received.

Elemental analyses were done by M. Magna (CNRS, Toulouse) for C and H and by the Service Central de Microanalyse du CNRS (Lyon) for the remaining elements.

Infrared spectra were recorded on a Perkin-Elmer 983 spectrometer as Nujol mulls prepared in the glovebox. The ^1H and ^{31}P NMR spectra were recorded at low temperature on a Bruker WH-90 spectrometer with THF-d_8 or CD_2Cl_2 as solvents. Chemical shifts were referenced to residual solvent signals for ^1H NMR (CD_2Cl_2, δ_H 5.33; THF-d_8, δ_H 1.90, 3.80) and to external

(1) Galdysz, J. A. *Adv. Organomet. Chem.* **1982**, *20*, 1.
(2) Thorn, D. L. *Organometallics* **1982**, *1*, 197. Thorn, D. L.; Roe, D. C. *Organometallics* **1987**, *6*, 617.
(3) Only a few cationic formyl complexes have been reported: Smith, G.; Cole-Hamilton, D. J. *J. Chem. Soc., Chem. Commun.* **1982**, 490. Smith, G.; Cole-Hamilton, D. J.; Thornton-Pett, M.; Hursthouse, M. B. *J. Chem. Soc., Dalton Trans.* **1983**, 2501. Smith, G.; Cole-Hamilton, D. J.; Thornton-Pett, M.; Hursthouse, M. B. *Polyhedron* **1983**, *2*, 1241. Barratt, D. S.; Cole-Hamilton, D. J. *J. Chem. Soc., Chem. Commun.* **1985**, 458. Lilga, M. A.; Ibers, J. A. *Organometallics* **1985**, *4*, 590.
(4) Clark, G. R.; Headford, C. E. L.; Marsden, K.; Roper, W. R. *J. Organomet. Chem.* **1982**, *231*, 335.
(5) Roper, W. R.; Wright, L. J. *J. Organomet. Chem.* **1982**, *234*, C5.
(6) Gambarotta, S.; Floriani, C.; Chiesi-Villa, A.; Guastini, C. *Organometallics* **1986**, *5*, 2425.
(7) Fahey, D. R. *J. Am. Chem. Soc.* **1981**, *103*, 136. Wood, C. D.; Garrou, P. E. *Organometallics* **1984**, *3*, 170.
(8) Wolfsberger, W.; Schmidbaur, H. *Synth. React. Inorg. Met. Org. Chem.* **1974**, *4*, 149.
(9) Klein, H. F.; Karsch, H. H. *Inorg. Chem.* **1975**, *14*, 473.

0276-7333/90/2309-1041$02.50/0

H_3PO_4 (62.5% in D_2O, δ 0) for ^{31}P NMR.

$[Co(PMe_3)_4]PF_6$. To $CoBr(PMe_3)_3$ (3 mmol, 1.1 g) in 20 mL of methanol were added 3 mmol of PMe_3 and 3 mmol (0.5 g) of $NaPF_6$. The violet solution immediately turned green. It was stirred for 0.5 h. Cooling at −80 °C overnight precipitated green crystals, which were filtered off, dried, and stored under argon; yield 90%. Anal. Calcd for $C_{12}H_{36}CoF_6P_5$: C, 28.36; H, 7.14. Found: C, 28.19; H, 7.08.

$[Co(PMe_3)_4]BPh_4$. To 2.7 mmol (1.0 g) of $CoBr(PMe_3)_3$ dissolved in 15 mL of acetonitrile were simultaneously added at −30 °C 2.7 mmol (0.9 g) of $NaBPh_4$ dissolved in 20 mL of methanol and 2.7 mmol of PMe_3. After 0.5 h stirring, green crystals precipitated. They were filtered off, dried, and kept under argon; yield 95%. Anal. Calcd for $C_{36}H_{56}BCoP_4$: C, 63.36% H, 8.27. Found: C, 63.20; H, 8.19.

$[Co(CO)(PMe_3)_4]PF_6$, 1. To a solution of $[Co(PMe_3)_4]PF_6$ (1.83 mmol, 0.93 g) in 15 mL of tetrahydrofuran was added 1.83 mmol of paraformaldehyde. The green solution was stirred at room temperature until it turned light orange. Cooling overnight at 5 °C precipitated orange crystals. They were filtered off, dried, and kept under argon; yield 85%. Anal. Calcd for $C_{13}H_{36}CoF_6OP_5$: C, 29.12; H, 6.77. Found: C, 29.08; H, 6.72. IR (Nujol mull) 1885 cm^{-1}, ν(CO); ^{31}P NMR (CD_2Cl_2, 188K) −5.5 ppm (s). The reaction was not affected by adding formaldehyde as an aqueous solution or by using excess formaldehyde (CH_2O/Co ratio = 1.75) in either form.

$[CoH_{2-2x}(CO)_x(PMe_3)_4]BPh_4$, 2. To a solution of 0.7 g (1.0 mmol) of $[Co(PMe_3)_4]BPh_4$ dissolved in tetrahydrofuran (20 mL) was added excess solid paraformaldehyde (1.75 mmol). The resulting suspension was stirred for 4 h at room temperature until the green solution turned orange red. The solution was filtered to remove undissolved formaldehyde. Cooling overnight at 5 °C precipitated orange–red crystals, which were filtered off, dried, and kept under argon; yield 65%. Anal. Calcd (assuming the composition deduced from X-ray work, x = 0.42, see below) for $C_{36.42}H_{57.16}BCoO_{0.42}P_4$: Co, 8.28; P, 17.82; B, 1.55; C, 62.90; H, 8.18. Found: Co, 8.11; P, 17.50; B, 1.52; C, 62.69; H, 8.03.

More orange–red crystals were obtained from a second crystallization at 5 °C. However, when the filtrate was cooled at −10 °C, a mixture of **2** and of yellow crystals precipitated. Elemental analysis and the infrared spectrum identified these yellow crystals as $[Co(CO)(PMe_3)_4)]BPh_4$. When the reaction was conducted with an aqueous solution of paraformaldehyde, the solution changed color very quickly. After stirring for 0.5 h, the solution was cooled to 5 °C and **2** precipitated as observed above.

$[CoD_{2-2x}(CO)_x(PMe_3)_4]BPh_4$. The compound was prepared as for **2** from solid paraformaldehyde (98% ^2H). Orange–red crystals precipitated at 5 °C overnight; yield 60%.

$[CoH_{2-2x}(^{13}CO)_x(PMe_3)_4]BPh_4$. The compound was prepared as for **2**. The 90% ^{13}C-labeled paraformaldehyde was added as a 26% aqueous suspension.

$[Co(CO)(PMe_3)_4]BPh_4$, 3. An equimolecular amount of CO gas (1.5 mmol) was allowed to react with 1.46 mmol (1.0 g) of $[Co(PMe_3)_4]BPh_4$ dissolved in 20 mL of tetrahydrofuran. The solution, which immediately turned yellow, was stirred for 0.5 h. Cooling overnight at −10 °C precipitated yellow crystals, which were filtered off, dried, and kept under argon; yield 60%. Anal. Calcd for $C_{37}H_{56}BCoOP_4$: C, 62.55; H, 7.94; B, 1.52; Co, 8.29; P, 17.44. Found: C, 62.99; H, 8.13; B, 1.56; Co, 8.48; P, 17.83. IR (Nujol) 1890 cm^{-1}, ν(CO); ^{31}P NMR (THF-d_8, 188 K) −6 ppm (s).

$[CoH_2(PMe_3)_4]BPh_4$. Molecular hydrogen was bubbled in a tetrahydrofuran solution (15 mL) of $[Co(PMe_3)_4]BPh_4$ (1.46 mmol, 1.0 g) for 2 h. A light green solution resulted. Cooling at −25 °C precipitated a light yellow powder, which was filtered off, dried and kept under argon; yield 53%. Anal. Calcd for $C_{36}H_{58}BCoP_4$: C, 63.17; H, 8.54; Co, 8.61; P, 18.10; B, 1.58. Found: C, 63.30; H, 8.50; Co, 8.61; P, 18.13; B, 1.58. IR (Nujol) 1956, 1938 cm^{-1}, ν(CoH); ^{31}P NMR (THF-d_8, 188 K) 2 ppm (br, d); ^1H NMR (THF-d_8, 188 K) −14.7 ppm (dt, J_{HP_a} = 63 Hz, J_{HP_e} = 34 Hz).

Structure Determination of $[Co(CO)(PMe_3)_4]PF_6$: $C_{13}H_{36}CoF_6OP_5$; fw = 536.22; monoclinic, $P2_1/n$, a = 11.280 (4), b = 14.948 (5), c = 14.088 (7) Å, β = 90.69 (3)°, Z = 4, D_c = 1.499 g cm^{-3}. λ(Mo K$\bar{\alpha}$) = 0.710 69 Å, μ = 10.99 cm^{-1}, F(000) = 112, T = 169 K.

A roughly spherical, deep orange specimen ($r \approx 0.15$ mm) was scraped clean from some soft amorphous pale purple material resulting from surface decomposition. It was glued to the tip of a glass fiber, mounted on an Enraf-Nonius CAD-4diffractometer, and quickly brought down to −104 °C. Cell parameters were determined on the basis of 25 centered reflections (20.7° ≤ 2θ ≤ 28.3°) and axial photographs verified a monoclinic cell. The Niggli matrix unambiguously showed that no higher symmetry was present. The intensities were measured at low temperature by using a bisecting $\omega/2\theta$ scan at 1.7° min^{-1} scan rate over (1.00 + 0.35 tan θ) degrees for the hkl and $\bar{h}kl$ octants. Seven standard reflections measured every hour showed a fluctuation within ±2.6%. A total of 3972 reflections were collected, $2\theta_{max}$ = 45.0°. Systematic extinctions determined $P2_1/n$ as the space group. Lorentz and polarization corrections were applied. No absorption correction was necessary ($\mu r \approx 0.16$). Removal of negative or zero intensity reflections resulted in 2912 unique reflections, of which 2340 with $I > 3\sigma(I)$ were used for structure determination.

The structure was determined with the SHELX package.[10] The position of the Co atom was found by automated direct methods. P and C atoms were subsequently found on a Fourier difference (ΔF) map. Six F atoms were added to the model, with fixed F–P–F angles. The following ΔF map revealed a second orientation of the PF_6^- anion. The two individuals were refined together, each with fixed octahedral geometry, giving occupancy factors of 0.54 (1) and 0.46 (1). All of the hydrogen atoms were then observed on the next ΔF map. They were refined positionally, with a common temperature factor. The geometry restrictions on the PF_6^- anions were then removed, and all nonhydrogen atoms were allowed to refine anisotropically. For the final cycles, the F and H atoms were fixed. The least-squares refinement was done on $\sum w(|F_o| - |F_c|)^2$, with $w = (\sigma^2(F) + 0.0004F^2)^{-1}$, giving R = 0.029, R_w = 0.035, and S = 1.227. The final average and maximum values of (Δ/σ) were 0.007 and 0.036, respectively. The final ΔF map showed a general background within ±0.28 e $Å^{-3}$.

Structure Determination of $[Co(H_2,CO)(PMe_3)_4]BPh_4$: $C_{36.42}H_{57.16}BCoO_{0.42}P_4$; fw = 695.41; monoclinic, $P2_1$, a = 15.985 (6), b = 12.512 (5), c = 20.410 (9), β = 111.76 (3)°, V = 3791.2 $Å^3$, D_c = 1.218 g cm^{-3}, Z = 4, λ(Mo K$\bar{\alpha}$) = 0.710 69 Å (graphite monochromator), μ(Mo Kα) = 6.4 cm^{-1}, T = 293 K.

A specimen of dimensions 0.29 × 0.11 × 0.44 mm^3 was cut from a large block and introduced into a Lindemann capillary filled with nitrogen. Laue symmetry and cell parameters were determined by indexing 25 random reflections centered in the counter of an Enraf-Nonius CAD-4 diffractometer. The cell was checked by means of long-exposure axial photographs, which showed appropriate layer line spacings. A mirror plane on the films obtained for the 12.51-Å axis confirmed the monoclinic Laue symmetry. The Niggli matrix unambiguously showed that no higher symmetry was present.

A total of 5211 independent hkl and $hk\bar{l}$ reflections were collected as described above (Mo K$\bar{\alpha}$, 2θ ≤ 45°). The three standard reflections fluctuated within ±2.1% during the experiment. A set of 4369 measurements with $I > 3\sigma(I)$ was retained for structure determination. These data were corrected for the Lorentz effect, polarization, and absorption (Gaussian integration, transmission range = 0.78–0.86). Inspection of the full data set for systematic absences revealed only one condition ($0k0$, $k \neq 2n$), which was consistent with space groups $P2_1$ and $P2_1/m$.

The structure was solved by the heavy-atom method. The Patterson map was first interpreted in the centric $P2_1/m$ space group. It was consistent with the presence of two independent pairs of Co atoms occupying crystallographic mirror planes (equipoint e). Two P atoms also lying on these mirrors could be located at this stage. However, the difference Fourier (ΔF) map phased on this model revealed only poorly defined positions for the remaining P atoms. Introducing these new positions into the phasing model yielded a ΔF map containing only some of the BPh_4^- atoms, with erratic bond lengths. This centric model was abandoned, and structure resolution was undertaken in the noncentric $P2_1$ space group.

In this space group, two pairs of Co atoms occupy general equipoints. The y coordinate of Co1 was used to fix the origin

(10) Sheldrick, G. M. SHELX-76, Crystallographic Program System; University of Cambridge, UK, 1976.

along *b*. Co2 and the P atoms properly carried over from the centric group were then refined for a few cycles. Co2 moved slightly, but significantly, from the pseudo mirror plane, while the P positions adjusted, so that the next ΔF map revealed positions for most of the atoms in the two independent BPh_4^- ions, as well as some of the phosphine methyl carbons. The missing BPh_4^- and phosphine carbons were found in the next ΔF map, which also contained electron density properly oriented to correspond to a CO ligand bound to each cobalt. The CO groups were introduced into the structure with full occupancies at this point. The structure was refined isotropically (full-matrix) and convergence was reached for $R = \sum||F_o| - |F_c||/\sum|F_o| = 0.131$ and $R_w = [\sum w(|F_o| - |F_c|)^2/\sum w|F_o|^2]^{1/2} = 0.144$. The temperature factors for the CO ligands were all above 17 Å^2, and they did not decrease when the remaining non-hydrogen atoms were anisotropically refined (block-diagonal least squares, $R = 0.063$, $R_w = 0.073$). It was concluded that the CO sites were only partially occupied. At this stage, occupancy factors of 0.50 were arbitrarily assigned. The hydrogen atoms, most of which were visible in the ΔF map, were introduced at idealized positions (C–H = 0.95 Å). Those of the phenyl rings (sp^2 hybridization) were assigned isotropic temperature factors $B = 3.2$ Å^2. For the methyl groups, idealized sp^3 positions were calculated to give optimum fit with the peaks observed in the map ($B = 4.0$ Å^2). Hydrogen parameters were not refined, but the coordinates were recalculated after each least-squares cycle. Refinement including hydrogen contributions reduced R to 0.049 and R_w to 0.060.

At this point, the SHELX package[10] was used to refine occupancy factors for CO. The coordinates of C1, C2, O1, and O2 were independently refined, but a common occupancy factor was assigned for the C and O atom of each CO ligand. Also, constraints were applied in the refinement to keep the temperature factors of C1 and C2 equal. The O1 and O2 pair was similarly handled. Refinement led to occupancies of 0.30 (3) for C1–O1 and 0.54 (3) for C2–O2. These values were not varied for the rest of the refinement, but the constraints on the CO temperature factors were removed. A few extra cycles (non-hydrogen atoms anisotropic, fixed hydrogen contributions) led to $R = 0.048$ and $R_w = 0.059$. The 10 highest peaks in the ΔF map (0.46–0.65 e Å^{-3}) were within 0.8 Å from a Co atom, except for a peak of 0.54 e Å^{-3} at 1.55 Å from Co1, near the middle of the 140.8° P2–Co1–P3 angle. Since spectroscopic results were consistent with the presence of $[Co(CO)(PMe_3)_4]^+$ and $[CoH_2(PMe_3)_4]^+$ cations, this peak was attributed to a hydride ligand. The second Co1–H bond is probably oriented roughly in the same direction as the Co–CO bond, so that electron density originating from the 0.70 H atom could not be found near the 0.30 C atoms of the CO ligand. The absence of individual electron density regions near Co2 is not surprising, since the higher occupancy of C2–O2 (0.54) requires occupancies of only 0.46 for the hydrides. Peaks of this height would be lost in the general background.

The H1 hydride atom was added to the model (occupancy factor = 0.70) and a few extra cycles were calculated, which did not significantly change the results for the rest of the structure. The final agreement factors are $R = 0.048$, $R_w = 0.059$, and the goodness-of-fit ratio is 2.42. The general background in the ΔF map is ±0.45 e Å^{-3}, except for the above-mentioned peaks near Co.

The scattering curves, as well as the f' and f'' contributions to anomalous dispersion for Co and P, were from standard sources.[11] The programs used, other than SHELX,[10] are listed elsewhere.[12] The coordinates for both compounds are listed in Table I.

Results and Discussion

In THF solution, the PF_6^- salt of $[Co(PMe_3)_4]^+$ reacts rapidly with HCHO, introduced either as solid paraformaldehyde or aqueous solution, with evolution of H_2, to afford the carbonyl complex $[Co(CO)(PMe_3)_4]PF_6$ (1):

$$[Co(PMe_3)_4]PF_6 + CH_2O \rightarrow \underset{\mathbf{1}}{[Co(CO)(PMe_3)_4]PF_6} + H_2$$

Formation of hydrido complexes $[CoH_2(PMe_3)_4]PF_6$ or $[CoH(PMe_3)_4]$ is not observed. This is in good agreement with the known behavior of cationic cobalt complexes, where the presence of a positive charge on the metal dramatically reduces the probability of hydrogen addition relative to phosphine or carbon monoxide addition.[13] This is well illustrated by the isoelectronic Fe(0) complexes.[14] Moreover, the $[CoH_2(P(OMe)_3)_4]^+$ complex, when isolated, readily looses H_2 via an intramolecular process, giving rise to the $[Co(P(OMe)_3)_4]^+$ species.[15]

Using the BPh_4^- salt[16] produces orange–red crystals of the nonstoichiometric compound $[CoH_{2-2x}(CO)_x(PMe_3)_4]BPh_4$ (**2**), which is the only product isolated when the solution is left at 5 °C overnight. However, on cooling the solution at −10 °C, a mixture of **2** and of yellow crystals of $[Co(CO)(PMe_3)_4]BPh_4$ (**3**) precipitates. Infrared spectra show the presence of these two complexes. The yield of **3** increases when the solution is kept at 20 °C several days before precipitation occurs.

Compound **1** can be handled in air for a short time. Its structure, determined by single-crystal X-ray diffraction (vide infra), indicates the presence of isolated PF_6^- anions and $[Co(CO)(PMe_3)_4]^+$ cations showing a distorted trigonal bipyramid structure with CO occupying an equatorial site. The strong infrared absorption at 1885 cm^{-1} corresponds to the ν(CO) mode of the equatorial CO ligand. The molecule is fluxional at 188 K as indicated by the single ^{31}P NMR signal at −5.5 ppm.

A TBP structure with equatorial CO for compound **3** is deduced from its similar infrared ν(CO) band at 1890 cm^{-1} and ^{31}P NMR signal at −6 ppm.

Compound **2** presents a strong vibration in its infrared spectrum (Nujol mull) at 1945 cm^{-1}, with a shoulder at 1955 cm^{-1}. This absorption is in the range of the Co–H stretching frequencies (1938, 1956 cm^{-1}) of $[CoH_2(PMe_3)_4]BPh_4$[17,18] but appears at higher energy than ν(CO) for the trigonal-bipyramidal compound $[Co(CO)(PMe_3)_4]PF_6$ (1885 cm^{-1}). Labeling experiments with CD_2O and $^{13}CH_2O$ (Table II) clearly show that the 1945-cm^{-1} band includes ν(CO) of a terminal axial monocarbonyl species and ν(CoH) of a dihydridocobalt(III) complex. Furthermore, NMR studies indicate that in solution, the spectrum of **2** results from the superposition of the spectra of $[Co(CO)(PMe_3)_4]^+$ (TBP with CO equatorial) and $[CoH_2(PMe_3)_4]^+$. The fluxional $[Co(CO)(PMe_3)_4]BPh_4$ compound is characterized by the NMR equivalence of the phosphines giving a singlet at −6 ppm ($J_{P^{13}C} = 12$ Hz). In the ^{31}P NMR spectrum of $[CoH_2(PMe_3)_4]^+$ at −100 °C, there are two broad doublets which are temperature dependent between +20 and −100 °C. The ^1H NMR spectrum shows a doublet of triplets ($J_{HP_a} = 63$ Hz, $J_{HP_e} = 34$ Hz) which turns into a singlet at −14.7 ppm by ^{31}P decoupling. All these data are consistent with the results obtained from $[CoH_2(PMe_3)_4]BPh_4$ prepared independently and, more generally, with d^8 $MH_2(PR_3)_4$ compounds.[19]

(11) Cromer, D. T.; Waber, J. T. *Acta Crystallogr.* **1965**, *18*, 104. Stewart, R. F.; Davidson, E. R.; Simpson, W. T. *J. Chem. Phys.* **1965**, *42*, 3175. Cromer, D. T. *Acta Crystallogr.* **1965**, *18*, 17.

(12) Authier-Martin, M.: Beauchamp, A. L. *Can. J. Chem.* **1977**, *55*, 1213.

(13) Pérès, Y.; Kerkeni, A.; Dartiguenave, M.; Dartiguenave, Y.; Bélanger-Gariépy, F.; Beauchamp, A. L. *J. Organomet. Chem.* **1987**, *323*, 397.

(14) Harris, T. V.; Rathke, J. W.; Muetterties, E. L. *J. Am. Chem. Soc.* **1979**, *100*, 6966.

(15) Muetterties, E. L.; Watson, P. L. *J. Am. Chem. Soc.* **1976**, *98*, 4665.

(16) Ananias de Carvalho, L. C.; Dartiguenave, M.; Dartiguenave, Y.; Beauchamp, A. L. *J. Am. Chem. Soc.* **1984**, *106*, 6848.

(17) Bressan, M.; Rigo, P. *Inorg. Chem.* **1978**, *17*, 769.

(18) Misono, A.; Uchida, Y.; Hidai, M.; Kuse, T. *J. Chem. Soc., Chem. Commun.* **1968**, 981.

Table I. Positional Coordinates (×10⁴; Co, P × 10⁵) and Equivalent Isotropic Temperature Factors (Å² × 10³)

atom	x	y	z	U_{eq}	atom	x	y	z	U_{eq}
				$[Co(CO)(PMe_3)_4]PF_6$					
Co	25857 (4)	16163 (3)	82806 (3)	18	F5B[a]	2519 (28)	1020 (17)	3495 (17)	113
P1	8467 (8)	23529 (6)	83406 (6)	23	F6B[a]	3647 (28)	53 (28)	2639 (30)	69
P2	25424 (8)	13091 (6)	98173 (6)	25	O1	3279 (3)	−246 (2)	8193 (2)	45
P3	40889 (8)	25985 (6)	83847 (6)	23	C1	2972 (3)	499 (3)	8223 (2)	30
P4	26235 (8)	15018 (6)	67112 (6)	22	C11	−376 (3)	1829 (3)	8981 (3)	39
P5	25047 (9)	171 (6)	32914 (7)	28	C12	913 (3)	3468 (3)	8864 (3)	37
F1A[a]	3112 (13)	−488 (11)	4120 (10)	78	C13	−4 (3)	2640 (3)	7273 (3)	43
F2A[a]	2288 (25)	−869 (14)	2778 (15)	109	C21	3962 (4)	955 (3)	10315 (3)	40
F3A[a]	1239 (25)	−59 (15)	3782 (22)	49	C22	1642 (4)	324 (3)	10083 (3)	46
F4A[a]	1926 (24)	574 (22)	2487 (17)	90	C23	2050 (3)	2104 (3)	10722 (3)	35
F5A[a]	2776 (22)	944 (13)	3808 (13)	83	C31	4255 (3)	3436 (3)	7444 (3)	34
F6A[a]	3728 (22)	144 (22)	2765 (25)	49	C32	4220 (3)	3338 (2)	9421 (3)	32
F1B[a]	3342 (15)	−154 (12)	4185 (8)	80	C33	5570 (3)	2095 (3)	8385 (3)	38
F2B[a]	2447 (29)	−1010 (15)	3080 (15)	80	C41	1612 (3)	651 (3)	6262 (3)	34
F3B[a]	1415 (31)	−55 (20)	3975 (26)	52	C42	2307 (3)	2432 (3)	5892 (3)	35
F4B[a]	1636 (28)	183 (25)	2396 (15)	80	C43	4039 (3)	1109 (3)	6247 (3)	33
				$[Co(H_2/CO)(PMe_3)_4]BPh_4$					
Co1	21698 (7)	25000	−11994 (5)	41	C62	6361 (5)	2383 (6)	−2899 (4)	36
Co2	23292 (8)	24208 (9)	38220 (5)	50	C63	6291 (5)	2283 (6)	−3604 (4)	39
P1	12038 (13)	24279 (17)	−22862 (11)	35	C64	7035 (5)	2153 (6)	−3765 (4)	39
P2	24898 (13)	41969 (15)	−11372 (11)	27	C65	7888 (5)	2081 (6)	−3208 (4)	32
P3	16450 (12)	12995 (14)	−6948 (10)	23	C66	7925 (5)	2162 (6)	−2530 (4)	29
P4	33061 (14)	17620 (20)	−14122 (12)	47	C71	6568 (4)	3230 (6)	−1377 (4)	27
P5	12949 (14)	25034 (20)	27404 (12)	45	C72	6319 (5)	3143 (6)	−806 (4)	35
P6	24647 (13)	6836 (16)	38755 (10)	28	C73	5832 (5)	3930 (7)	−625 (4)	34
P7	16591 (13)	35238 (16)	43087 (11)	31	C74	5553 (4)	4844 (6)	−1022 (4)	29
P8	33918 (15)	32001 (19)	35405 (13)	51	C75	5798 (5)	4955 (6)	−1602 (4)	36
O1[b]	3849 (10)	2387 (12)	234 (8)	29	C76	6294 (5)	4159 (6)	−1776 (4)	37
O2[c]	3854 (6)	2460 (10)	5231 (5)	55	C81	8254 (4)	2773 (5)	−958 (4)	24
C1[b]	3253 (15)	2454 (21)	−323 (13)	32	C82	8641 (4)	2406 (7)	−273 (4)	39
C2[c]	3259 (8)	2501 (11)	4681 (6)	27	C83	9415 (5)	2807 (7)	216 (4)	47
C11	7052 (5)	3795 (6)	3602 (4)	29	C84	9859 (6)	3631 (8)	48 (4)	56
C12	7731 (5)	4570 (6)	3846 (4)	34	C85	9499 (5)	4035 (7)	−619 (5)	51
C13	7553 (5)	5631 (6)	3871 (4)	37	C86	8705 (5)	3659 (6)	−1131 (4)	38
C14	6678 (6)	5967 (6)	3668 (5)	44	CP1	1547 (5)	2767 (8)	−3019 (4)	50
C15	5978 (5)	5233 (7)	3451 (5)	51	CP2	240 (5)	3297 (8)	−2478 (5)	51
C16	6192 (6)	4149 (7)	3436 (4)	45	CP3	662 (6)	1118 (8)	−2619 (6)	65
C21	7192 (4)	2560 (5)	2653 (3)	22	CP4	1681 (6)	5104 (7)	−900 (5)	56
C22	6347 (4)	2464 (6)	2082 (4)	30	CP5	2515 (5)	4920 (6)	−1879 (4)	41
C23	6273 (5)	2564 (6)	1396 (4)	38	CP6	3513 (6)	4636 (7)	−465 (4)	43
C24	7049 (6)	2705 (6)	1239 (4)	45	CP7	1856 (6)	−82 (7)	−778 (5)	56
C25	7850 (5)	2761 (6)	1757 (4)	40	CP8	418 (5)	1319 (7)	−932 (5)	40
C26	7932 (4)	2675 (5)	2470 (4)	28	CP9	2014 (6)	1403 (6)	243 (4)	46
C31	6552 (4)	1703 (5)	3624 (4)	26	CP10	3876 (5)	2544 (8)	−1883 (5)	57
C32	6304 (4)	1792 (6)	4211 (3)	25	CP11	3149 (5)	516 (8)	−1918 (5)	57
C33	5812 (5)	1028 (6)	4415 (4)	35	CP12	4231 (6)	1440 (10)	−590 (6)	86
C34	5553 (5)	128 (7)	3999 (4)	42	CP13	1614 (5)	2136 (6)	1997 (4)	40
C35	5761 (5)	−19 (6)	3418 (4)	39	CP14	331 (7)	1675 (9)	2578 (6)	73
C36	6260 (4)	746 (6)	3235 (4)	29	CP15	745 (6)	3767 (8)	2387 (4)	57
C41	8235 (5)	2074 (7)	4028 (4)	35	CP16	1698 (6)	−27 (7)	4121 (4)	58
C42	8633 (5)	2503 (6)	4717 (4)	36	CP17	2474 (7)	−49 (6)	3088 (4)	50
C43	9420 (5)	2026 (9)	5197 (4)	58	CP18	3522 (7)	218 (8)	4535 (5)	65
C44	9820 (5)	1173 (8)	5007 (6)	67	CP19	1866 (5)	4951 (6)	4219 (5)	41
C45	9417 (5)	730 (7)	4331 (5)	46	CP20	456 (6)	3542 (8)	4087 (5)	58
C46	8665 (5)	1237 (6)	3887 (4)	37	CP21	2020 (6)	3397 (8)	5281 (5)	60
C51	7046 (4)	1136 (6)	−1365 (3)	25	CP22	3931 (5)	2378 (7)	3077 (4)	47
C52	7700 (5)	341 (7)	−1151 (4)	36	CP23	3141 (7)	4400 (6)	3025 (5)	61
C53	7491 (6)	−729 (7)	−1093 (4)	47	CP24	4397 (7)	3732 (10)	4232 (6)	109
C54	6600 (5)	−1068 (7)	−1291 (4)	44	B1	7251 (5)	2531 (7)	3491 (4)	27
C55	5940 (5)	−325 (6)	−1547 (4)	41	B2	7277 (5)	2349 (7)	−1527 (4)	24
C56	6147 (4)	736 (6)	−1589 (4)	32	H1[d]	1250	2799	−1160	
C61	7199 (4)	2372 (6)	−2328 (4)	33					

Occupancy factors: [a] 0.5; [b] 0.30; [c] 0.54; [d] 0.70.

To get information on these compounds in the solid state, namely, to identify the type of Co–CO bonds and understand the high frequency of the ν(CO) band for **2**, X-ray diffraction work was carried out.

Crystallographic Work. The structure and atom labeling of the $[Co(CO)(PMe_3)_4]^+$ cation in the PF_6^- compound are shown in Figure 1. Selected interatomic distances and bond angles are listed in Table III. The complex exhibits normal carbonyl and trimethylphosphine monocoordination, with the carbonyl ligand occupying an equatorial position in a distorted trigonal bipyramid. On the opposite side, the presence of four PMe_3 ligands creates

(19) Tebbe, F. N.; Meakin, P.; Jesson, J. P.; Muetterties, E. L. *J. Am. Chem. Soc.* **1970**, *92*, 1068. Meakin, P.; Muetterties, E. L.; Jesson, J. P. *J. Am. Chem. Soc.* **1972**, *95*, 75. Meakin, P.; Guggenberger, L. J.; Jesson, J. P.; Gerlach, D. H.; Tebbe, F. N.; Peet, W. G.; Muetterties, E. L. *J. Am. Chem. Soc.* **1970**, *92*, 3482.

Table II. Infrared Data (cm^{-1}, Nujol Mull)

	ν(CO)	ν(CoH)
$[CoH_{2-2x}(CO)_x(PMe_3)_4]BPh_4$	1945	1955 sh
$[CoH_{2-2x}(^{13}CO)_x(PMe_3)_4]BPh_4$	1900	1955, 1940
$[CoD_{2-2x}(CO)_x(PMe_3)_4]BPh_4$	1945	1400, 1385
$[CoH_2(PMe_3)_4]BPh_4$		1956, 1938
$[Co(CO)(PMe_3)_4]BPh_4$	1890	
$[Co(CO)(PMe_3)_4]PF_6$	1885	

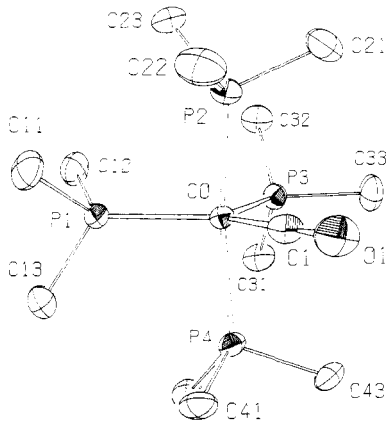

Figure 1. ORTEP drawing for the complex cation in $[Co(CO)(PMe_3)_4]PF_6$ (1). The Co atom has a slightly distorted trigonal-bipyramidal environment with CO in the equatorial position. The thermal ellipsoids are drawn at 50% probability. The hydrogen atoms are omitted for simplicity.

steric strain, which is reduced by the axial phosphines being displaced away from the equatorial ones and toward the smaller CO ligand. The resulting P2–Co–P4 angle is 163.60 (4)°. The staggered orientation of both axial phosphines with respect to the equatorial bonds allows one of the P–CH_3 bonds in each axial phosphine to lie above the bisector of the P3–Co–P1 angle, where steric hindrance is minimum. Nevertheless, some repulsion is experienced by these P–CH_3 bonds, since the Co–P–C angles are found to be ~11° greater than the corresponding angles for the methyl groups on the CO side.

Significant differences are found for the Co–P distances between the axial (mean 2.216 Å) and the equatorial bonds (mean 2.249 Å). These values agree with those observed for the $[Co(CO)_2(PMe_3)_3]^+$ cation.[13] However, the present Co–CO distance (1.728 (4) Å) is found to be shorter than those of the above cation (1.740 (6) and 1.766 (5) Å). This reflects the fact that Co–CO bond stabilization by metal-to-ligand π-bonding does not have to be shared by two CO ligands as in the $[Co(CO)_2(PMe_3)_3]^+$ complex.

The disordered PF_6^- ion can be seen in Figure A-1 (supplementary material; see the paragraph at the end of the paper). Although the anion could be resolved in two orientations, the shapes of the thermal ellipsoids suggest the presence of further disorder, tending toward $D_{\infty h}$ point symmetry with the C_∞ axis along the [F13,F23]–P–[F16,F26] direction.

A packing diagram (Figure A-2, supplementary material) shows that the lattice is held together by normal ionic and van der Waals forces.

The unit cell of the nonstoichiometric $[Co(H_2/CO)(PMe_3)_4]BPh_4$ complex contains four BPh_4^- ions and two independent pairs of sites occupied by cationic cobalt complexes each containing four PMe_3 ligands. On each of these sites are found two types of complex cations (Figure 2). The cobalt(I) species $[Co(CO)(PMe_3)_4]^+$ is found on type 1 sites 30% of the time and on type 2 sites 54% of the time. The species present the rest of the time is the cis-octahedral dihydrido Co(III) cation $[CoH_2(PMe_3)_4]^+$. The absence of large thermal ellipsoids or satellite electron density peaks indicates that the PMe_3 ligands in the $Co(PMe_3)_4$ fragments are coincident, or nearly so, for both species on any crystallographic site. The amount of $[Co(CO)PMe_3)_4]^+$ on each type of sites was determined by refinement of the CO occupancy factors.

The $[Co(CO)(PMe_3)_4]^+$ cation has a distorted trigonal-bipyramid structure. The axial sites are occupied by phosphines P1 (cation 1) or P5 (cation 2) and by CO ligands (Figure 2). The CO molecules are linearly bonded

Table III. Interatomic Distances and Bond Angles for $[Co(CO)(PMe_3)_4]PF_6$

Distances, Å			
Co–P1	2.252 (1)	P4–C42	1.839 (4)
Co–P2	2.214 (1)	P4–C43	1.830 (4)
Co–P3	2.246 (1)	C–O	1.168 (5)
Co–P4	2.219 (1)	P–F11[a]	1.54 (1)
Co–C	1.728 (4)	P–F12	1.53 (2)
P1–C11	1.832 (4)	P–F13	1.60 (3)
P1–C12	1.824 (4)	P–F14	1.54 (3)
P1–C13	1.826 (4)	P–F15	1.59 (2)
P2–C21	1.819 (4)	P–F16	1.59 (3)
P2–C22	1.830 (4)	P–F21	1.59 (1)
P2–C23	1.833 (4)	P–F22	1.57 (2)
P3–C31	1.834 (4)	P–F23	1.57 (4)
P3–C32	1.836 (4)	P–F24	1.61 (3)
P3–C33	1.833 (4)	P–F25	1.53 (2)
P4–C41	1.817 (4)	P–F26	1.59 (4)
Angles, deg			
P1–Co–P2	92.02 (4)	Co–P2–C23	123.8 (1)
P1–Co–P3	109.58 (4)	C21–P2–C22	100.1 (2)
P1–Co–P4	95.87 (4)	C21–P2–C23	101.2 (2)
P1–Co–C	134.0 (1)	C22–P2–C23	101.9 (2)
P2–Co–P3	95.58 (4)	Co–P3–C31	118.9 (1)
P2–Co–P4	163.60 (4)	Co–P3–C32	119.9 (1)
P2–Co–C	81.6 (1)	Co–P3–C33	114.8 (1)
P3–Co–P4	95.27 (4)	C31–P3–C32	98.9 (2)
P3–Co–C	116.4 (1)	C31–P3–C33	100.4 (2)
P4–Co–C	82.6 (1)	C32–P3–C33	100.5 (2)
Co–P1–C11	118.1 (1)	Co–P4–C41	112.4 (1)
Co–P1–C12	115.5 (1)	Co–P4–C42	124.1 (1)
Co–P1–C13	122.3 (1)	Co–P4–C43	114.1 (1)
C11–P1–C12	102.7 (2)	C41–P4–C42	101.2 (2)
C11–P1–C13	96.6 (2)	C41–P4–C43	101.4 (2)
C12–P1–C13	97.9 (2)	C42–P4–C43	100.5 (2)
Co–P2–C21	114.1 (1)	Co–C–O	177.3 (3)
Co–P2–C22	112.7 (1)		

[a] All F atoms have half occupancies.

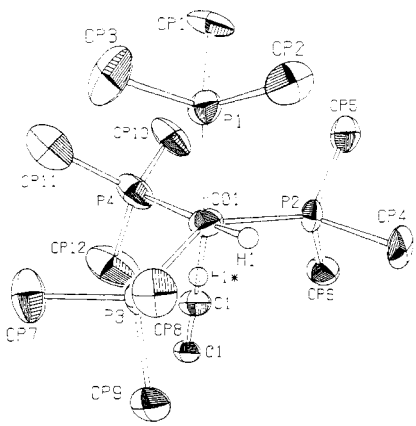

Figure 2. ORTEP drawing of the cations found on type 1 sites in $[CoH_{2-2x}(CO)_x(PMe_3)_4]BPh_4$ (2). Ellipsoids correspond to 50% probability. The $Co(PMe_3)_4$ fragment is common to both species, whose occupancy factors are 30% for $[Co(CO)(PMe_3)_4]^+$ (trigonal bipyramid with axial CO) and 70% for $[CoH_2(PMe_3)_4]^+$ (cis-octahedral coordination). The open spheres represent the probable positions of the hydride ligands in the $[CoH_2(PMe_3)_4]^+$ ion. Cations with the same composition and similar geometry are also disordered on sites of type 2.

Table IV. Interatomic Distances and Bond Angles in $[Co(H_2/CO)(PMe_3)_4]BPh_4$

	Distances, Å		
Co1-P1	2.185 (2)	Co2-P5	2.216 (3)
Co1-P2	2.177 (2)	Co2-P6	2.183 (2)
Co1-P3	2.159 (2)	Co2-P7	2.197 (2)
Co1-P4	2.219 (3)	Co2-P8	2.211 (3)
Co1-C1[a]	1.98 (2)	Co2-C2[c]	1.83 (2)
Co1-H1[b]	1.55	C2[c]-O2[c]	1.17 (2)
C1[a]-O1[a]	1.18 (3)	P5-CP13	1.829 (8)
P1-CP1	1.824 (9)	P5-CP14	1.783 (12)
P1-CP2	1.806 (10)	P5-CP15	1.823 (10)
P1-CP3	1.860 (10)	P6-CP16	1.732 (10)
P2-CP4	1.913 (10)	P6-CP17	1.855 (9)
P2-CP5	1.777 (9)	P6-CP18	1.822 (11)
P2-CP6	1.788 (9)	P7-CP19	1.838 (8)
P3-CP7	1.781 (9)	P7-CP20	1.805 (11)
P3-CP8	1.838 (9)	P7-CP21	1.857 (9)
P3-CP9	1.786 (9)	P8-CP22	1.817 (9)
P4-CP10	1.833 (9)	P8-CP23	1.791 (9)
P4-CP11	1.835 (10)	P8-CP24	1.826 (12)
P4-CP12	1.823 (11)		
	Angles, deg		
P1-Co1-P2	99.3 (1)	P5-Co2-P6	96.9 (1)
P1-Co1-P3	101.7 (1)	P5-Co2-P7	96.5 (1)
P1-Co1-P4	96.1 (1)	P5-Co2-P8	94.7 (1)
P1-Co1-C1[a]	166.0 (7)	P5-Co2-C2[c]	172.3 (4)
P2-Co1-P3	140.8 (1)	P6-Co2-P7	131.2 (1)
P2-Co1-P4	103.0 (1)	P6-Co2-P8	112.4 (1)
P2-Co1-C1[a]	82.4 (7)	P6-Co2-C2[c]	88.5 (4)
P3-Co1-P4	107.1 (1)	P7-Co2-P8	113.0 (1)
P3-Co1-C1[a]	85.0 (7)	P7-Co2-C2[c]	83.8 (4)
P4-Co1-C1[a]	70.1 (7)	P8-Co2-C2[c]	78.2 (4)
Co1-C1[a]-O1[a]	174 (2)	Co2-C2[c]-O2[c]	174 (1)
Co1-P1-CP1	120.6 (3)	Co2-P5-CP13	118.7 (3)
Co1-P1-CP2	114.9 (3)	Co2-P5-CP14	115.6 (4)
Co1-P1-CP3	117.7 (3)	Co2-P5-CP15	120.4 (3)
CP1-P1-CP2	100.0 (4)	CP13-P5-CP14	100.8 (5)
CP1-P1-CP3	98.4 (4)	CP13-P5-CP15	97.6 (4)
CP2-P1-CP3	101.9 (4)	CP14-P5-CP15	100.0 (5)
Co1-P2-CP4	115.3 (3)	Co2-P6-CP16	117.2 (3)
Co1-P2-CP5	121.7 (3)	Co2-P6-CP17	118.8 (3)
Co1-P2-CP6	118.2 (3)	Co2-P6-CP18	113.8 (3)
CP4-P2-CP5	98.3 (4)	CP16-P6-CP17	103.3 (4)
CP4-P2-CP6	97.8 (4)	CP16-P6-CP18	100.6 (5)
CP5-P2-CP6	101.2 (4)	CP17-P6-CP18	100.3 (4)
Co1-P3-CP7	120.6 (3)	Co2-P7-CP19	115.4 (3)
Co1-P3-CP8	115.5 (3)	Co2-P7-CP20	123.2 (3)
Co1-P3-CP9	115.4 (3)	Co2-P7-CP21	114.8 (3)
CP7-P3-CP8	102.1 (4)	CP19-P7-CP20	100.2 (4)
CP7-P3-CP9	100.0 (4)	CP19-P7-CP21	101.2 (4)
CP8-P3-CP9	100.2 (4)	CP20-P7-CP21	98.6 (4)
Co1-P4-CP10	118.8 (3)	Co2-P8-CP22	116.4 (3)
Co1-P4-CP11	120.8 (3)	Co2-P8-CP23	119.7 (3)
Co1-P4-CP12	110.8 (4)	Co2-P8-CP24	120.0 (4)
CP10-P4-CP11	98.6 (4)	CP22-P8-CP23	102.4 (4)
CP10-P4-CP12	102.1 (5)	CP22-P8-CP24	99.1 (5)
CP11-P4-CP12	103.0 (5)	CP23-P8-CP24	95.2 (5)
H1[b]-Co1-P1	75	H1[b]-Co1-P4	167
H1[b]-Co1-P2	88	H1[b]-Co1-C1	119
H1[b]-Co1-P3	66		

[a] Occupancy factor 0.30. [b] Occupancy factor 0.70. [c] Occupancy factor 0.54.

(Table IV), thereby ruling out the presence of CO as a formyl unit, which should have a Co–C–O angle near 120°.[21] The Co–P distances (2.159–2.219 Å, σ = 0.003 Å) are in the range observed for $[Co(CO)_2(PMe_3)_3]BPh_4$.[13] The $[Co(CO)(PMe_3)_4]^+$ ion found in the above PF_6^- salt also shows a trigonal-bipyramid structure, but in contrast with the cation observed here, the CO ligand is found to be equatorial. The preference of CO for equatorial positions in a d^8 trigonal bipyramid system arises from more efficient back-bonding compared to axial sites.[20] However, the presence of bulky ligands can displace the small CO ligands to axial sites in order to open for the bulkier ligand equatorial sites where the large 120° angles leave more space. For instance, the structures of two related $[Fe(CO)_2(SO_2)(PR_3)_2]$ compounds are known:[22] the PR_3 ligands are axial when R is phenoxide, but they displace CO to axial sites and replace them in equatorial sites when R is the bulkier *o*-methylphenoxide group. To our knowledge, the present $[Co(CO)(PMe_3)_4]^+$ cation is the first example for which the two isomeric forms have been isolated and crystallographically characterized.

Cobalt dihydrido compounds are known in the literature,[23] although no crystallographic studies have yet been performed on such systems. The Co-H1 distance (1.55 Å) is not accurate, but it is comparable with those found for other cobalt complexes containing nonbridging hydrides.[24] It is well-known that a hydride ligand does not fill much space around the metal.[24] The coordination polyhedra of hydrido complexes are often distorted to allow the bulkier ligands to be displaced toward the hydride region. This effect is observed in the present case (Table IV): the P1–Co1–P and P5–Co2–P angles are all greater than 90°, whereas the P2–Co1–P3 and P6–Co2–P7 angles, which should be 180° in an ideal octahedron, are respectively 140.8 (1) and 131.2 (1)°. This pattern of distortions is very similar to the one found for $FeH_2[PPh(OEt)_2]_4$.[26]

A packing diagram is shown in Figure 3. Anions of type 1 and of type 2 in alternance form rows along the *c* direction. Alternance of both types of cations also defines rows parallel to those of the anions. Pairs of rows of opposite charges are repeated in adjacent cells in the *a* and in the *b* directions, so that any row of one ion is surrounded by four rows of the opposite ion. Cohesion originates from normal van der Waals contacts between these large ions. The BPh_4^- ions are not disordered, and their mutal interactions remain the same whichever cation is present on any given site. As to the cation–cation and cation–BPh_4^- interactions, they are probably almost insensitive to the particular cation present: most of the cationic surface consists of phosphine methyl groups occupying the same positions in both kinds of cations, whereas the Co–H_2 or Co–CO regions cover only a small fraction of the surface. To cocrystallize in the structure observed here, the two cations had to adopt similar van der Waals envelopes. The dihydride can be regarded as the rigid species controlling the size and shape of the cationic sites in the crystal. The *cis*-$[CoH_2(PMe_3)_4]^+$ and the ground-state equatorial-CO-$[Co(CO)(PMe_3)_4]^+$ ions would have van der Waals envelopes too different to share a crystal site. However, rearrangement of $[Co(CO)(PMe_3)_4]^+$ into the axial-CO isomer is likely to be fast for such a fluxional molecule and not energetically costly. Therefore, stabilization of the axial-CO isomer can be regarded as resulting from cocrystallization in a host lattice mainly determined by the BPh_4 and the more rigid and slightly more abundant dihydride

(20) Rossi, A. R.; Hoffmann, R. *Inorg. Chem.* **1975**, *14*, 365.
(21) Wayland, B. B.; Woods, B. A.; Pierce, R. *J. Am. Chem. Soc.* **1982**, *104*, 302. Casey, C. P.; McAlister, D. R.; Calabrese, J. C.; Neumann, S. M.; Andrews, M. A.; Miszaros, M. W.; Haller, K. J. *Cryst. Struct. Commun.* **1982**, *11*, 1015. Wong, W. K.; Tam, W.; Strouse, C. E.; Gludysz, J. A. *J. Chem. Soc., Chem. Commun.* **1979**, 530.
(22) Conway, P.; Grant, S. M.; Manning, A. R.; Stephens, F. S. *Inorg. Chem.* **1983**, *22*, 3714.
(23) Archer, N. J.; Haszeldine, R. N.; Parish, R. V. D. *J. Chem. Soc., Dalton Trans.* **1979**, 695. Janowicz, A. H.; Bergman, R. G. *J. Am. Chem. Soc.* **1981**, *103*, 2488. Muetterties, E. L.; Hirsekorn, F. J. *J. Am. Chem. Soc.* **1974**, *96*, 7920.
(24) Ghilardi, C. A.; Midollini, S.; Sacconi, L. *Inorg. Chem.* **1975**, *14*, 1790. Titus, D. D.; Orio, A. A.; Marsh, R. E.; Gray, H. B. *J. Chem. Soc., Chem. Commun.* **1971**, 322. Sacconi, L.; Ghilardi, C. A.; Mealli, C.; Zanobini, F. *Inorg. Chem.* **1975**, *14*, 380.
(25) Tolman, C. A. *Chem. Rev.* **1977**, *77*, 313.
(26) Guggenberger, L. J.; Titus, D. D.; Flood, M. T.; Marsh, R. E.; Orio, A. A.; Gray, H. B. *J. Am. Chem. Soc.* **1972**, *94*, 1135.

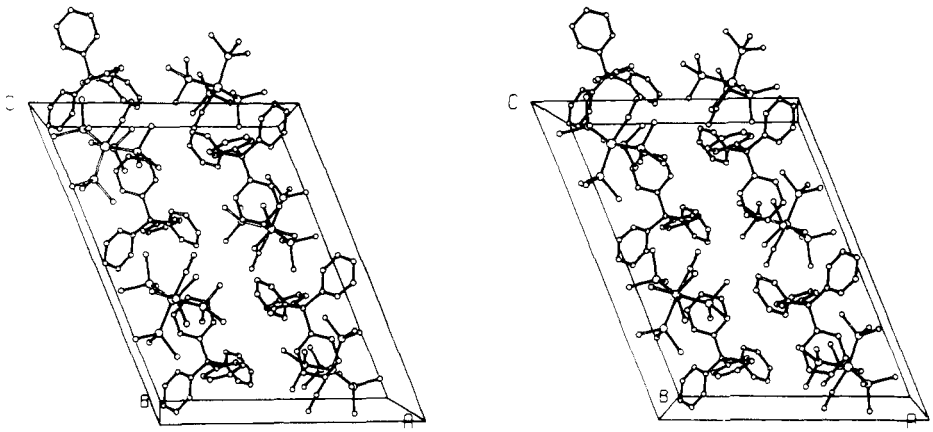

Figure 3. Stereoview of the unit cell of $[CoH_{2-2x}(CO)_x(PMe_3)_4]BPh_4$ (**2**). The BPh_4^- ions are ordered. The cationic sites are occupied by $[Co(CO)(PMe_3)_4]^+$ or $[CoH_2(PMe_3)_4]^+$ ions as shown in Figure 2. For simplicity, the structure is represented with all cationic sites occupied by $[Co(CO)(PMe_3)_4]^+$ ions.

complex. However, it is difficult to rationalize the presence of two crystallographically independent sites with different populations in the lattice.

Conclusion

Decomposition of formaldehyde does occur on cationic cobalt(I) complexes, and it is found to be counterion dependent. Loss of CO, which is the recognized mode of decomposition for a number of formyl complexes, is not the major decomposition route observed here.

The PF_6^- salt gives rise to loss of H_2, leading exclusively to the equatorial-CO form of $[Co(CO)(PMe_3)_4]^+$. In agreement with this, we cannot isolate a hydrogen adduct of $[Co(PMe_3)_4]PF_6$ in the solid state, and there is no evidence for its presence in solution from spectroscopic results.

The simultaneous presence of the $[Co(CO)(PMe_3)_4]^+$ and $[CoH_2(PMe_3)_4]^+$ cations when $[Co(PMe_3)_4]PBh_4$ is used suggests the existence of two competitive decomposition pathways: loss of CO and loss of H_2. This is supported by the ability of $[Co(PMe_3)_4]BPh_4$ to add H_2 oxidatively and give $[CoH_2(PMe_3)_4]BPh_4$, whereas this is not observed with $[Co(PMe_3)_4]PF_6$.

The first step of the reaction of CH_2O on the cationic Co compounds probably generates a hydridoformyl cobalt cation by oxidative addition of CH_2O on the cobalt center. No experimental evidence for such a species is available, but iridium and osmium analogues are known and present similar decomposition pathways. The decomposition of osmium formyl complexes is particularly informative. $Os(CH_2O)(CO)_2(PPh_3)_2$ decomposes at 40 °C to form both $OsH_2(CO)_2(PPh_3)_2$ and $Os(CO)_3(PPh_3)_2$ in roughly equimolecular ratio. Although the CO loss remains the most general pathway, Roper et al. have observed that loss of H_2 is favored when a hydrido ligand is present in the osmium coordination sphere as observed in $Os(CHO)H(CO)_2(PPh_3)_2$.[4,5]

Trigonal-bipyramid compounds usually yield only one isolable stereoisomer. In this study, both the axial-CO and equatorial-CO forms of the $[Co(CO)(PMe_3)_4]^+$ cation are observed and crystallographically characterized. IR data show that the normal equatorial-CO isomer found in the PF_6^- salt is also present in the stoichiometric BPh_4^- salt. Hence, stabilization of the axial-CO form in the nonstoichiometric material is predominantly a solid-state effect and requires the presence of the dihydride complex. However, the possibility of observing this isomer under the present conditions is in agreement with the general belief that the axial-CO form is not much higher in energy than the equatorial-CO ground-state structure.[20]

Acknowledgment. We thank M. J. Olivier for collecting the X-ray data. Support of this research through the Conseil de Recherches en Sciences Naturelles et en Génie du Canada and the Programme d'Échanges Interuniversitaires Franco-québecois is gratefully acknowledged.

Supplementary Material Available: Listings of thermal parameters and hydrogen coordinates for $[Co(CO)(PMe_3)_4]PF_6$ and $[CoH_{2-2x}(CO)_x(PMe_3)_4]BPh_4$ (18 pages); listings of structure factors (30 pages). Ordering information is given on any current masthead page.